

# A new approach to measuring high-resolution magnetic Compton profiles

 H. Kawata,<sup>a\*</sup> H. Sakurai,<sup>b</sup> N. Shiotani<sup>a</sup> and Y. Watanabe<sup>c</sup>

 Received 29 August 2005  
 Accepted 5 December 2005

<sup>a</sup>Photon Factory, Institute of Materials Structure Science, High Energy Accelerator Research Organization, Tsukuba, Ibaraki 305-0801, Japan, <sup>b</sup>Department of Electronic Engineering, Faculty of Engineering, Gunma University, Kiryu, Gunma 376-8515, Japan, and <sup>c</sup>Institute of Industrial Science, University of Tokyo, Meguro, Tokyo 153-0805, Japan. E-mail: hiroshi.kawata@kek.jp

It is demonstrated that long-term stability in the polarization of incident photons delivered from an insertion device makes it possible to measure magnetic Compton profiles with a momentum resolution of 0.15 atomic units or better, without employing a solid-state detector and the traditional method of reversing the external magnetic field or the handedness of the polarization of incident photons in an asynchronous cycle with a short period of tens to hundreds of seconds.

 © 2006 International Union of Crystallography  
 Printed in Great Britain – all rights reserved

**Keywords:** Compton scattering; electron momentum density; magnetic Compton profile; high-resolution measurements.

## 1. Introduction

Magnetic Compton profile measurements yield information about the direction with respect to bulk magnetization and magnitude of the electron spin magnetization of ferromagnetic and ferrimagnetic materials. Furthermore, the uniqueness of the method is in providing the characteristics of the wavefunctions of spin-unpaired electrons through the observed momentum distribution (see, for example, Cooper *et al.*, 2004, for an overview of Compton scattering). The Compton profile  $J(p_z)$  of the ferromagnetic state and magnetic Compton profile  $J_{\text{mag}}(p_z)$  are defined in terms of the electron momentum densities of majority-spin electrons  $n_{\text{up}}(\mathbf{p})$  and that of minority-spin electrons  $n_{\text{down}}(\mathbf{p})$ ,

$$J(p_z) = \iint [n_{\text{up}}(\mathbf{p}) + n_{\text{down}}(\mathbf{p})] dp_x dp_y \quad (1)$$

and

$$J_{\text{mag}}(p_z) = \iint [n_{\text{up}}(\mathbf{p}) - n_{\text{down}}(\mathbf{p})] dp_x dp_y, \quad (2)$$

where  $p_x$ ,  $p_y$  and  $p_z$  are the Cartesian momentum components, the  $z$  axis being parallel to the scattering vector. The double-differential scattering cross section is related to  $J(p_z)$  and  $J_{\text{mag}}(p_z)$  by

$$\frac{d^2\sigma}{d\Omega dE_f} = \left(\frac{d\sigma}{d\Omega}\right)_{\text{charge}} \left(\frac{E_f}{E_i}\right) J(p_z) + \left(\frac{d\sigma}{d\Omega}\right)_{\text{mag}} \left(\frac{E_f}{E_i}\right) J_{\text{mag}}(p_z), \quad (3)$$

where  $E_{i(f)}$  is the initial (final) photon energy. The first term in the right-hand side of (3) is the scattering cross section due to electron charges and independent of electron spins. From the literature, the cross section in the second term is given by

$$\left(\frac{d\sigma}{d\Omega}\right)_{\text{mag}} = (-r_0^2/mc^2) P_c (1 - \cos\varphi) \mathbf{S} \cdot (\mathbf{k}_i \cos\varphi + \mathbf{k}_f), \quad (4)$$

where  $r_0$  is the classical electron radius,  $P_c$  is the degree of circular polarization of the incident photons,  $\varphi$  is the scattering angle,  $\mathbf{S}$  is the electron spin and  $\mathbf{k}_{i(f)}$  is the wavevector of the incident (scattered) photon. The Compton profile of the ferromagnetic state can be obtained by adding data sets taken with the magnetization direction ( $\mathbf{S}$ ) or photon polarization handedness ( $P_c$ ) reversed, while the magnetic Compton profile can be obtained by subtracting the data sets. The second term in the right-hand side of (3) is smaller than the first term by approximately a factor  $(E_i/mc^2) \times$  (number of spin unpaired electrons/total number of electrons). With  $E_i = 60$  keV, even for pure Fe the factor becomes  $1 \times 10^{-2}$   $[(60 \text{ keV}/511 \text{ keV}) \times (2.2/26)]$ . The measurement of the magnetic Compton profile, therefore, requires a very high statistical accuracy. For this reason almost all magnetic Compton profiles reported so far were measured by using a Ge solid-state detector for energy analysis of scattered photons and by reversing the external magnetic field in an asynchronous cycle with a period of tens to hundreds of seconds. The frequent reversal of the external magnetic field or the handedness has been employed in order to reduce the effects of any beam decay and fluctuation in intensity and in polarization, and long-term drift in electronic circuits for data acquisition. The use of a Ge solid-state detector is almost inevitable for attaining a high statistical accuracy, but it gives a momentum resolution of 0.4 atomic units (a.u.) at best. A resolution of 0.4 a.u. is high enough to discuss the direction and magnitude of spin magnetization and overall character of the wavefunction of unpaired electrons. It is, however, not high enough to reveal band structure effects and details of the

Fermi surface signatures. A successful exception is a report (Sakurai *et al.*, 1994) of a high-resolution magnetic Compton profile of  $\text{Fe}_{0.942}\text{Si}_{0.058}$ . Instead of using a Ge solid-state detector they used a high-resolution spectrometer (Sakurai *et al.*, 1992) which has a Cauchois-type crystal analyzer and a pair of image plates as a detector. The pair of image plates was rotated on every reversal of magnetization of the specimen so that the profile of one direction of magnetization was always recorded on the same image plate.

In this report we demonstrate that long-term stability in the polarization of incident photons delivered from an insertion device makes it possible to measure magnetic Compton profiles with a resolution of 0.15 a.u. or better, without employing a solid-state detector and the traditional way of reversing the external magnetic field in an asynchronous cycle with a short period. Since this is a demonstrative work we choose a commonly found Fe–Si single crystal as our specimen.

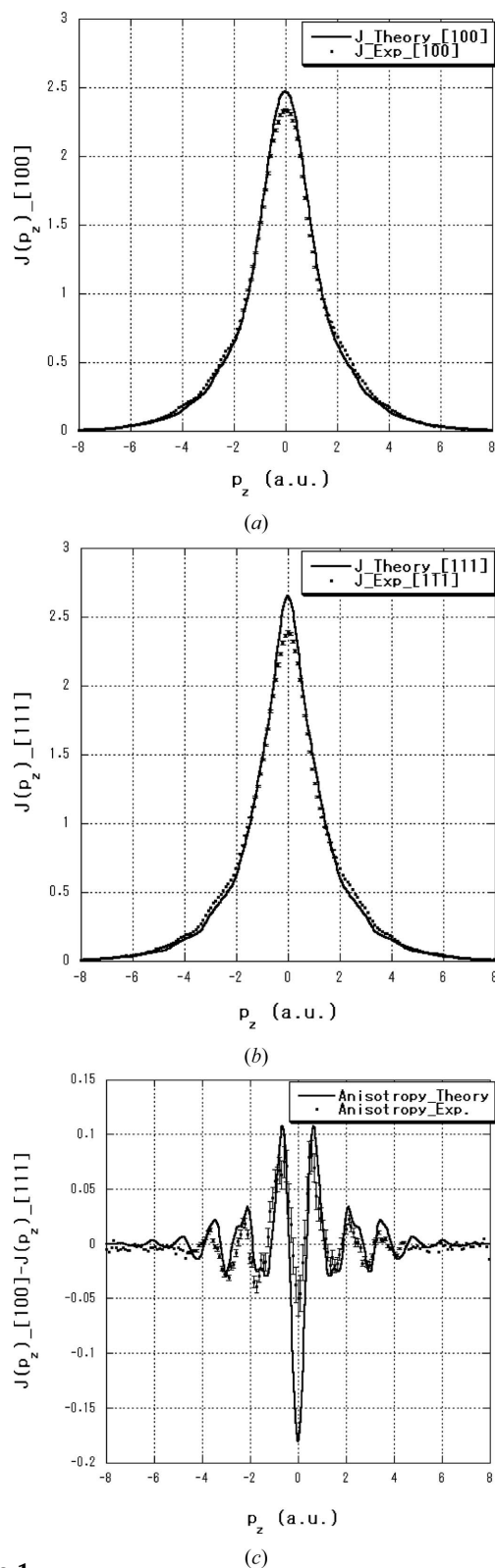
## 2. Experiment

The measurements were carried out at beamline NE1 of the 6.5 GeV KEK-PF-AR. The half-life of the ring current is about 20 h. Injection is performed twice or three times a day. The elliptic multipole wiggler (Yamamoto & Kitamura, 1987; Yamamoto *et al.*, 1989) delivers elliptically polarized photons of  $P_c = 0.40$ . The energy of incident photons is 59.1 keV. It has been proven by Kawata *et al.* (2003) with their real-time circular polarization monitor that the degree of circular polarization of incident photons delivered from the insertion device is constant for many hours. The specimen is a single-crystal plate of  $\text{Fe}_{0.942}\text{Si}_{0.058}$ , the thickness of which is 0.2 mm. The energy analysis of Compton-scattered photons is carried out by the same high-resolution spectrometer, but with one image plate, as Sakurai *et al.* (1994) used. The overall momentum resolution is mainly determined by an energy resolution of the monochromator and in this study it is 0.15 a.u. The specimen is clipped across the pole pieces of a C-shaped electromagnet. One measurement for one direction of magnetization lasts 8–12 h depending on the period of injection. After each run of 8–12 h the image plate is transferred to an image-plate reader. For each direction of magnetization the data of 80 h are stored and added. The total accumulated counts were  $9 \times 10^5$  at the Compton peak. To monitor the magnetic effect a Ge solid-state detector is placed along a direction different from the direction towards the image plate, but at the same scattering angle. Concerning the normalization of the data obtained by the image plate, first the magnetic effect, not the magnetic profile itself but the integrated area of it, observed by the Ge detector is obtained using the area under the quasi-elastic peak (about  $1 \times 10^9$  counts) for normalization. Then the magnetic effect is corrected for the difference in the angle between the magnetization and the scattering vector, and finally the corrected magnetic effect is used to normalize the data obtained by the image plate. The data are taken with an interval of approximately 0.02 a.u. In

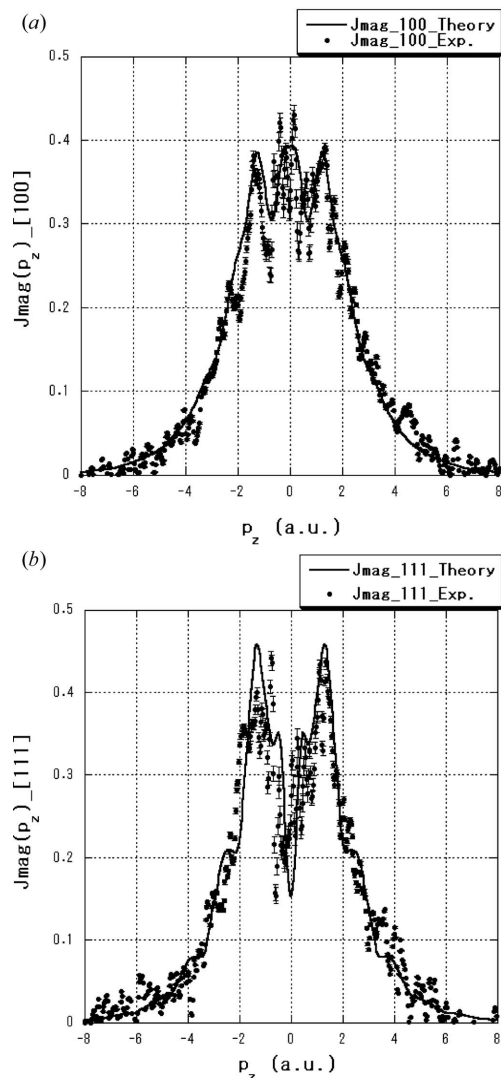
Fig. 1, to avoid busy figures, we plot them only every three data points. In Fig. 2 all the data points are plotted.

## 3. Results and discussion

Figs. 1(a) and 1(b) show  $J(p_z)$ , the profiles of the valence electrons of the ferromagnetic state along the [100] and [111] directions, respectively, and Fig. 1(c) shows the crystalline anisotropy, the difference of the two profiles in Figs. 1(a) and 1(b). Fig. 2 shows  $J_{\text{mag}}(p_z)$ , the magnetic profiles along the [100] (a) and [111] (b) directions. The full lines in Figs. 1 and 2 are the corresponding theoretical profiles for pure Fe computed by Kubo & Asano (1990) using the FLAPW method. The theoretical profiles are convoluted with the present experimental momentum resolution of 0.15 a.u. The number of valence electrons per atom is 7.77 for  $\text{Fe}_{0.942}\text{Si}_{0.058}$  and 8.0 for pure Fe; the number of magnetic electrons is 2.0 for  $\text{Fe}_{0.942}\text{Si}_{0.058}$  and 2.07 for pure Fe. The area under each curve is normalized accordingly. It is well known that the value of the magnetic moment per Fe atom in the Fe–Si alloy system remains the same as that of pure Fe as long as the concentration of Si is small. Therefore it is worth comparing the present results and the band theoretical predictions. Referring to Fig. 1, the overall shape of  $J(p_z)$  is well reproduced by the theory, in particular the fine structure beyond 2 a.u. Even taking into account the difference in the number of electrons per atom, the theoretical profiles are higher than the observed ones in small momenta and the situation is reversed in large momenta. This trend has always been found in studies of non-magnetic metals and alloys when comparison between band theory and experiment is made (*e.g.* Shiotani, 2004). The anisotropy is also well reproduced by the theory except that the theory gives larger anisotropy than the experiment, which is again commonly found in studies of metals and alloys. Although the total accumulated counts at the Compton peak are  $9 \times 10^5$  and the statistical accuracy is about  $1 \times 10^{-3}$ , the errors of our data points are determined not only by the number of accumulated counts but also by the non-uniformity of the image plate and inherent noise of the image-plate reader (Ito & Amemiya, 1991). Thus the observed magnetic profiles shown in Fig. 2 have larger error bars than those expected from the accumulated counts. This is one disadvantage of using an image plate as a detector. Another disadvantage is its poor detection efficiency. The image plate has, however, one big advantage over other detectors in that it has no electronic drift in the channel–energy relationship during the measurement. Successful installation of an X-ray CCD camera into the high-resolution Compton scattering spectrometer at SPring-8 (Itou & Sakurai, 2003) indicates that replacement of the image plate with an X-ray CCD camera is the most realistic solution of overcoming the disadvantages mentioned above. Referring to Fig. 2, the observed magnetic profiles reproduce most of the characteristics of the theoretical predictions. For the first time the sharp dip at  $p_z = 0$  a.u., the pronounced peak around 1.5 a.u. and the shoulder around 2.3 a.u. are observed in this study. Because of the rather large scatter of data points, however, it is not quite appropriate to


**Figure 1**

The Compton profiles of the valence electrons in the ferromagnetic state of  $\text{Fe}_{0.942}\text{Si}_{0.058}$ , measured along the [100] direction (a), along the [111] direction (b), and the difference of the two profiles (c). The full lines are corresponding theoretical profiles of pure Fe computed by Kubo & Asano (1990) using the FLAPW method. The theoretical profiles are convoluted with the present experimental resolution of 0.15 a.u. The area under the experimental profiles is normalized to 7.7 electrons/atom, and that of the theoretical profiles gives 7.9 electrons/atom.


**Figure 2**

Magnetic Compton profiles of  $\text{Fe}_{0.942}\text{Si}_{0.058}$ , measured along (a) the [100] direction and (b) the [111] direction. The full lines are corresponding theoretical profiles of pure Fe computed by Kubo & Asano (1990). The area under the experimental profile is normalized to 2.0 electrons/atom, and that of the theoretical profile is 2.07 electrons/atom. The theoretical profiles are convoluted with the present experimental resolution of 0.15 a.u.

give a quantitative discussion on whether there is any effect of adding Si on the band structure of pure Fe or not.

The high-resolution measurement described here should not be taken as a replacement of the conventional measurement with a Ge solid-state detector. Even in the case of Fe, it takes 20 times longer time for the high-resolution measurement to achieve the same statistical accuracy as that of the measurement with a Ge solid-state detector. The data obtained by the high-resolution measurement, however, are useful for precisely checking the predictions made by various theories on the band structure and the Fermi surface, the signature of which normally appears as fine structure on the magnetic profile.

In summary, we have demonstrated that the long-term stability in the polarization of incident photons delivered from

an insertion device makes it possible to measure magnetic Compton profiles with a resolution of 0.15 a.u. or better, without employing the traditional method of reversing the external magnetic field in an asynchronous cycle with a short period.

The authors are very grateful to Professor Kubo for providing the theoretical profiles of pure Fe. The measurements were performed with the approval of the Photon Factory Advisory Committee, proposal No. 2004G215.

### References

- Cooper, M. J., Mijnders, P. E., Shiotani, N., Sakai, N. & Bansil, A. (2004). Editors. *X-ray Compton Scattering*. Oxford University Press.
- Ito, M. & Amemiya, Y. (1991). *Nucl. Instrum. Methods Phys. Res. A*, **310**, 369–372.
- Itou, M. & Sakurai, Y. (2003). *Eighth International Conference on Synchrotron Radiation Instrumentation, AIP Conference Proceedings 705*, pp. 901–904. Melville, NY: AIP Press.
- Kawata, H., Adachi, H. & Matsumoto, I. (2003). *Eighth International Conference on Synchrotron Radiation Instrumentation, AIP Conference Proceedings 705*, pp. 549–552. Melville, NY: AIP Press.
- Kubo, Y. & Asano, S. (1990). *Phys. Rev. B*, **42**, 4431–4446.
- Sakurai, Y., Ito, M., Urai, T., Tanaka, Y., Sakai, N., Iwazumi, T., Kawata, H., Ando, M. & Shiotani, N. (1992). *Rev. Sci. Instrum.* **63**, 1190–1193.
- Sakurai, Y., Tanaka, Y., Ohata, T., Watanabe, Y., Nanao, S., Ushigami, Y., Iwazumi, T., Kawata, H. & Shiotani, N. (1994). *J. Phys. Condens. Matter*, **6**, 9469–9475.
- Shiotani, N. (2004). *X-ray Compton Scattering*, edited by M. J. Cooper, P. E. Mijnders, N. Shiotani, N. Sakai and A. Bansil, pp. 237–288. Oxford University Press.
- Yamamoto, S., Kawata, H., Kitamura, H., Ando, M., Sakai, N. & Shiotani, N. (1989). *Phys. Rev. Lett.* **62**, 2672–2675.
- Yamamoto, S. & Kitamura, H. (1987). *J. Appl. Phys.* **26**, L1613–L1615.